

A NEW ERA IN COSMOLOGY
ASP Conference Series, Vol. ???, 2001
T. Shanks & N. Metcalfe

Cepheids, Supernovae, H_0 , and the Age of the Universe

G. A. Tammann, B. Reindl, F. Thim

Astronomisches Institut der Universität Basel
Venusstrasse 7, CH-4102 Binningen, Switzerland

A. Saha

National Optical Astronomy Observatories
950 North Cherry Ave., Tucson, AZ 85726

A. Sandage

The Observatories of the Carnegie Institution of Washington
813 Santa Barbara Street, Pasadena, CA 91101

Abstract. The local expansion field is mapped using Cepheids, a complete sample of TF distances, and nearby cluster distances. The large-scale field is mapped using Cepheid-calibrated blue SNeIa. These data give $H_0(\text{local}) = 59.2 \pm 1.4 \text{ [km s}^{-1} \text{ Mpc}^{-1}]$ and $H_0(\text{cosmic}) = 57.4 \pm 2.3$. The intermediate expansion field ($1200 \leq v \lesssim 10000 \text{ km s}^{-1}$) is less well calibrated but fully consistent with $H_0 \approx 60$. H_0 is therefore (nearly) scale-invariant (high-density regions excluded). – The P-L relation of Cepheids is based on an improved zero point of $(m - M)_{\text{LMC}} = 18.56$. The slope of the P-L relation for $P > 10^d$, as judged from OGLE data (Udalski et al. 1999) is flatter than anticipated, which tends to increase the above values of H_0 by 3.4 units. No significant metallicity effect on the Cepheid distances seems to be indicated. For all practical purposes $H_0 = 60$ is recommended with a systematic error of probably less than 10%. – The corresponding expansion age is $T = 15.7 \pm 1.5 \text{ Gy}$ (with $\Omega_m = 0.3$, $\Omega_\Lambda = 0.7$), which compares well with the formation time of $15 \pm 2 \text{ Gy}$ for the apparently oldest globular cluster M 107.

1. Introduction

Cepheids and their P - L relation are the principal fundament of extragalactic distances (Section 2). Cepheid distances are available of nine galaxies which have produced blue SNeIa (Saha et al 2001 and references therein). Their resulting, very uniform luminosities can be applied to 35 more distant SNeIa ($v \lesssim 30000 \text{ km s}^{-1}$) to yield a first rate determination of the large-scale value of H_0 (Section 5). Details of the local expansion field are inserted in Section 3 and some remarks on the not so local expansion field in Section 4. The expansion age of the Universe is compared with independent age determination of old objects in the Galaxy in Section 6. Results and conclusions are compiled in Section 7.

2. Cepheids and their P-L relation

2.1. The shape of the P-L relation

The available Cepheid distances, which are useful for the extragalactic distance scale beyond the Local Group, are compiled in Table 1. The majority is derived from *HST* observations in V and I . All distances are based on the shape of the P - L relations by Madore & Freedman (1991)

$$M_V = -2.76 \log P - 1.46 \quad (1)$$

$$M_I = -3.06 \log P - 1.87 \quad (2)$$

As for the constant term see 2.2. Equations (1) and (2) yield apparent distance moduli μ_V and μ_I which, with $A_B = 4.1 E_{B-V}$, $A_V = 3.1 E_{B-V}$, and $A_I = 1.8 E_{B-V}$, give the true moduli

$$\mu^0 \equiv (m - M)^0 = 2.38\mu_I - 1.38\mu_V. \quad (3)$$

It may be noted that equations (1) and (2) imply $(V - I) \propto 0.3 \log P$. It was recently suggested (Freedman et al. 2001) that the OGLE photometry of Cepheids in LMC (Udalski et al. 1999) required a shallower relation $(V - I) \propto 0.2 \log P$, that long-period Cepheids were therefore intrinsically bluer than

Table 1. Adopted Cepheid Distance Moduli μ^0 [LMC at $\mu^0 = 18.56$].

Galaxy	v_{220}	$\Delta[\text{O}/\text{H}]^{**}$	$\mu^0 \dagger$	Src. [‡]	Galaxy	v_{220}	$\Delta[\text{O}/\text{H}]^{**}$	$\mu^0 \dagger$	Src. [‡]
NGC 224	LG	+0.50	24.47 (08)	5	NGC 3982	1497	—	31.78 (14)	1C
NGC 300	118	-0.15	26.68 (10)	5	NGC 4258	554	+0.35	29.55 (07)	5
NGC 598	LG	+0.30	24.64 (10)	5	NGC 4321	—	+0.65	31.02 (07)	5
NGC 925	790	+0.05	30.00 (04)	5	NGC 4414	660	+0.70	31.35 (15)	2C
NGC 1326A	1338	± 0.00	31.26 (10)	5	NGC 4496A	—	+0.25	31.09 (10)	1C
NGC 1365	1338	+0.45	31.42 (05)	5	NGC 4527	—	—	30.73 (15)	3
NGC 1425	1338	+0.50	31.73 (06)	5	NGC 4535	—	+0.70	31.09 (05)	5
NGC 2090	814	+0.30	30.50 (04)	5	NGC 4536	—	+0.35	31.16 (12)	1C
NGC 2403	365	+0.30	27.65 (24)	5	NGC 4548	—	+0.85	31.09 (05)	5
NGC 2541	802	± 0.00	30.48 (07)	5	NGC 4603	2323	—	32.67 (11)	6
NGC 3031	141	+0.25	27.89 (07)	5	NGC 4639	—	+0.50	32.09 (22)	1C
NGC 3198	861	+0.10	30.90 (08)	5	NGC 4725	—	+0.40	30.61 (06)	5
NGC 3319	955	-0.10	30.85 (09)	5	NGC 5253	153	-0.35	28.06 (07)	1C
NGC 3351	648	+0.75	30.04 (10)	5	NGC 5457	413	-0.13	29.36 (10)	5
NGC 3368	802	+0.70	30.21 (15)	4C	NGC 7331	1108	+0.15	30.96 (09)	5
NGC 3621	495	+0.15	29.29 (06)	5	IC 4182	330	-0.10	28.42 (12)	1C
NGC 3627	542	+0.75	30.28 (12)	1C					

^{*} Recession velocity corrected for Virgocentric infall (Kraan-Korteweg 1986). The velocities of the galaxies in the Virgo cluster region ($\alpha_{\text{M87}} < 30^\circ$) are not used in the following and are not shown.

^{**} $\Delta \log [\text{O}/\text{H}] = \log [\text{O}/\text{H}]_{\text{Gal}} - \log [\text{O}/\text{H}]_{\text{LMC}}$ derived from data given in Freedman et al. (2001)

[†] The errors in parentheses in units of $0^m.01$ are taken from the original sources. Some of them are unrealistically small. If the errors of the apparent moduli in V and I are optimistically assumed to be $\pm 0^m.05$, the errors of $(m - M)^0$ are $\gtrsim 0^m.15$ from equation (3). – Consequently the reliable maser distance $\mu^0 = 29.29 \pm 0.08$ of NGC 4258 (Herrnstein et al. 1999) is still in statistical agreement with the distance shown here.

[‡] C means the galaxy distance is used for the luminosity calibration of SNeIa.

Sources: (1) Saha et al. 2001; (2) Thim 2001; (3) mean of Saha et al. 2001 and Thim 2001; (4) mean of Tanvir et al. 1999 and source (5); (5) Freedman et al. 2001 (Table 3, column 2; including (small) corrections by excluding short-period Cepheids which may introduce selection bias); (6) Newman et al. 1999.

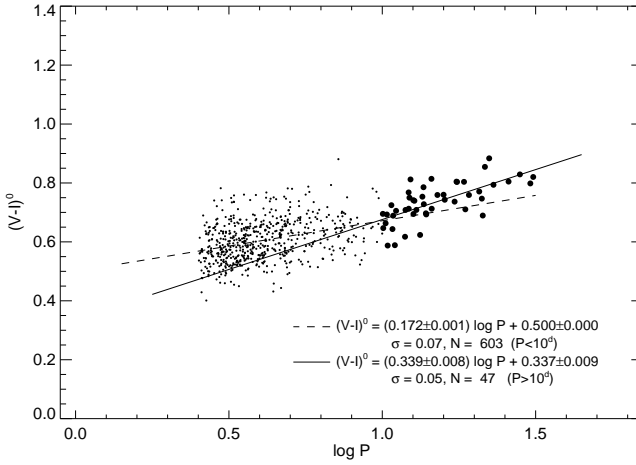


Figure 1. A $(V - I)$ vs. $\log P$ diagram of the fundamental-mode LMC Cepheids adopted by Udalski et al. (1999). Color excesses from that source. Small symbols: $P < 10^d$; large symbols: $P > 10^d$.

anticipated, and that the corresponding increase of the internal absorption would lead to a “dramatic” decrease of $\sim 0^m 14$ on average of those Cepheid distances in Table 1, which rely indeed on *long*-period Cepheids.

However, the data of Udalski et al. (1999) indicate a clear change of the $(V - I) - \log P$ relation near $P = 10$ days (Fig. 1), i.e. near the termination point of the Hertzsprung progression. While the slope is approximately 0.2 for $P < 10^d$, it steepens to $\gtrsim 0.3$ for $P > 10^d$. In fact the new data show Cepheids with $P > 10^d$ to be *redder* than implied by equations (1) and (2). (This statement holds if all Cepheid colors are consistently corrected by a constant LMC excess of $E_{B-V} = 0.1$. The color excesses given by Udalski et al. are variable and larger on average. Note that any possible overestimate of $\langle E_{B-V} \rangle$ of the LMC Cepheids affects the apparent moduli μ_V and μ_I of external galaxies, but *not* the true modulus from equation (3). Therefore the Udalski et al. values of $E(B - V)$ are adopted in the following without consequences for the derived distances).

The change of slope of the color relation in Fig. 1 demands a corresponding change of slope near $P = 10^d$ of the $M_V - \log P$ or of the $M_I - \log P$ relation or of both. Fits to the data for $P < 10^d$ and $P > 10^d$ give indeed significantly different slopes (Fig. 2):

$$P < 10 \text{ days} : M_V = (-2.862 \pm 0.002) \log P - (1.43 \mp 0.001); \quad (4)$$

$$M_I = (-3.034 \pm 0.001) \log P - (1.93 \mp 0.001) \quad (5)$$

$$P > 10 \text{ days} : M_V = (-2.487 \pm 0.025) \log P - (1.79 \mp 0.030); \quad (6)$$

$$M_I = (-2.825 \pm 0.019) \log P - (2.12 \mp 0.022) \quad (7)$$

Here $\mu_{\text{LMC}}^0 \equiv 18.56$ is assumed (cf. 2.2). Compared to equations (1) and (2) the equations (6) and (7) lead to smaller distance moduli by

$$\Delta\mu(P > 10^d) = -0.18 \log P + 0.14. \quad (8)$$

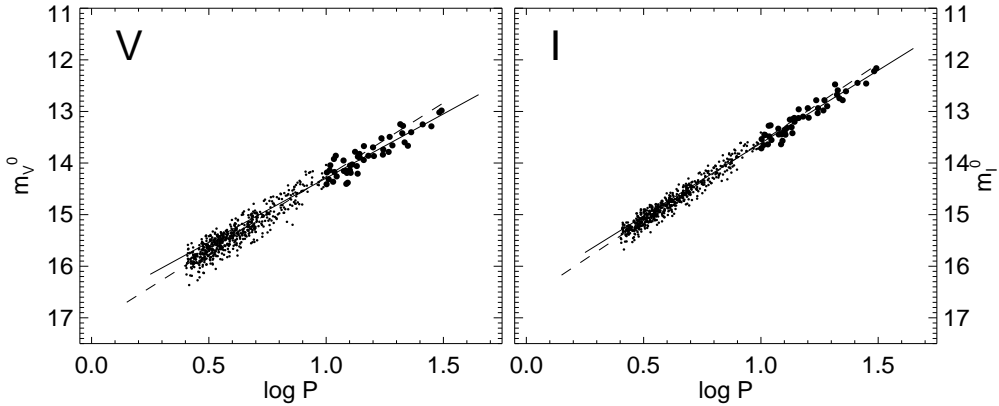


Figure 2. P - L relations in V and I of the fundamental-mode LMC Cepheids adopted by Udalski et al. (1999). Symbols like in Fig. 1.

This is not because Cepheids are bluer here (they have $(V - I) = 1.01$ at $\log P = 2$ in either case even with the large E_{B-V} values of Udalski et al.), but because the P - L relations are flatter for $P > 10^d$ than anticipated.

In the following the P - L relations of equation (1) and (2) are maintained because the data of Udalski et al. (1999) extend to only $P \leq 30$ days, while about half of the Cepheids in more distant galaxies have longer periods. However, the effect of the equations (6) and (7) – on the assumption that they can be extrapolated to longer periods – is taken up again in Section 7.

2.2. The zero point of the P-L relation

It is customary to set the zero point of the P - L relation by adopting $\mu_{\text{LMC}} = 18.50$. It is time now to improve this value. LMC moduli are compiled in Table 2 comprising a variety of methods with different, but poorly known systematic errors. A unweighted mean of $\mu_{\text{LMC}}^0 = 18.56$ is therefore adopted, which is used throughout this paper.

Red-clump stars and binaries were suggested to give rather low LMC moduli. Yet the most recent results agree statistically with the adopted value (cf. Table 1). Statistical parallaxes of Galactic RR Lyr stars, which pose formidable problems of sample selection, are given zero weight (cf. Walker 1999).

2.3. Metallicity effects of Cepheids?

The metal dependence of the P - L relation has so far not found a satisfactory solution from observations (e.g. Gould 1994; Sasselov et al. 1997; Kennicutt et al. 1998). Theoretical models give only a small effect (Chiosi et al. 1993; Saio & Gautschy 1998; Sandage et al. 1999; Alibert & Baraffe 2000; see however Caputo et al. 2000). If the model dependencies in V and I from Sandage et al. (1999, Fig. 3) are inserted into equation (3) one obtains a metal correction of $\Delta\mu = -0.12\Delta[\text{Fe}/\text{H}]$ in formal agreement with $-0.24 \pm 0.16\Delta[\text{O}/\text{H}]$ from Kennicutt et al. (1998). The rather marginal evidence from Fig. 3 has, however, the opposite sign. Moreover, the seven galaxies with Cepheid distances and

Table 2. The Distance Modulus of LMC

Reference	μ^0	Method
Sandage & Tammann (1971)	18.59	Galactic Cepheids in Clusters
Feast (1984)	18.50	Cepheids, OB, RR Lyrae, MS-fitting, Mira
Feast & Catchpole (1997)	18.70 ± 0.10	HIPPARCOS parallaxes of Galactic Cepheids
Van Leeuwen et al. (1997)	18.54 ± 0.10	HIPPARCOS parallaxes of Miras
Madore & Freedman (1998)	$18.44 - 18.57$	HIPPARCOS parallaxes of Galactic Cepheids
Panagia (1999)	18.58 ± 0.05	Ring around SN 1987A
Pont (1999)	18.58 ± 0.05	HIPPARCOS parallaxes of Galactic Cepheids
Walker (1999)	18.55 ± 0.10	Review
Feast (1999)	18.60 ± 0.10	Review
Walker (1992), Udalski et al. (1999)	18.53 ± 0.08	$M_V^{\text{RR}} = 0.41 \pm 0.07$ Sandage (1993), Chaboyer et al. (1998)
Groenewegen & Oudmaijer (2000)	18.60 ± 0.11	HIPPARCOS parallaxes of Galactic Cepheids
Kovács (2000)	18.52	Double mode RR Lyr
Sakai et al. (2000a)	18.59 ± 0.09	Tip of RGB
Cioni et al. (2000)	18.55 ± 0.04	Tip of RGB
Romaniello et al. (2000)	18.59 ± 0.09	Tip of RGB
Groenewegen & Salaris (2001)	18.42 ± 0.07	Eclipsing binary
Girardi & Salaris (2001)	18.55 ± 0.05	Red clump stars
Baraffe & Alibert (2001)	$18.60 - 18.70$	Pulsation theory of Cepheids
Adopted	18.56 ± 0.02	

known $\Delta[\text{O}/\text{H}]$ in Table 1, for which also SNe Ia distances can be determined based on a *mean* M^{corr} value (equation (13) below), give $-0.03 \pm 0.04\Delta[\text{O}/\text{H}]$ with a fortuitously small error. Even if the coefficient was as large as ± 0.25 the galaxy distances in Table 1 would be increased/decreased by only $0.^m08$ on average. No metallicity correction is applied in the following.

3. The Local Expansion Field ($v_{220} \lesssim 1200 \text{ km s}^{-1}$)

3.1. The local distance-calibrated Hubble diagram of Galaxies with Cepheid distances

The values $\log v_{220}$ of the galaxies in Table 1 are plotted versus their Cepheid distances μ^0 in Fig. 4. Galaxies within 30° of the Virgo cluster center are omitted because that region is noisy due to virial motions and infall from the cluster front- and back-sides.

If a Hubble line of slope 0.2 is fitted to the 23 galaxies with Cepheid distances, giving half weight to galaxies with $(m - M)^0 < 28.1$, one obtains

$$\log v = 0.2(m - M)^0 + a_0 \quad (9)$$

with $a_0 = -3.206 \pm 0.020$. Since $\log H_0 = a_0 + 5$, the local value of H_0 becomes $H_0 = 62.2 \pm 2.9 \text{ [km s}^{-1} \text{ Mpc}^{-1}\text{]}$.

The scatter about the Hubble line amounts to $\sigma_\mu = 0.^m43$, of which $\sigma_\mu = 0.^m15 - 0.^m20$ can be attributed to errors of the Cepheid moduli (cf. footnote in Table 1). The contribution to the scatter by peculiar velocities becomes then $\sigma_{\log v} \lesssim 0.08$ or $\Delta v_{\text{pec}}/v_{220} \lesssim 20\%$.

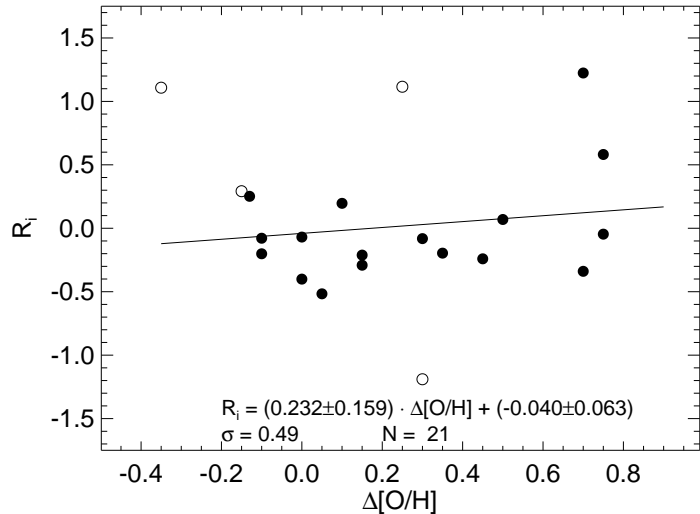


Figure 3. The dependence of Cepheid distances on the metallicity $\Delta[\text{O/H}] = [\text{O/H}]_{\text{Gal}} - [\text{O/H}]_{\text{LMC}}$. Plotted are the residuals R_i from the mean Hubble line in Fig. 4. Open symbols for galaxies with $\mu^0 < 28.1$ are given half weight.

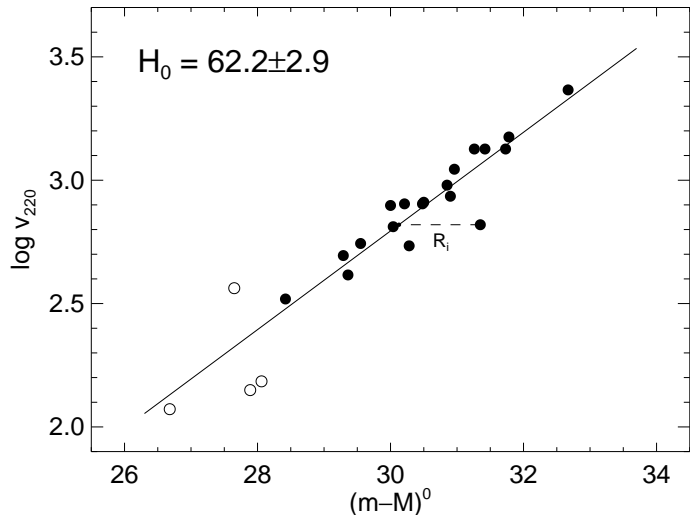


Figure 4. The distance-calibrated Hubble diagram plotting $\log v_{220}$ versus the Cepheid distance modulus of 23 galaxies. Open symbols are given half weight. The distance modulus residuals R_i are used in Fig. 3.

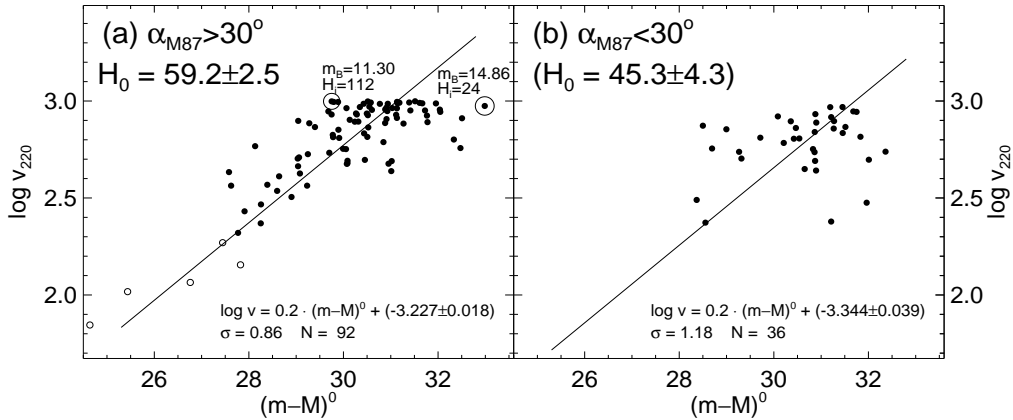


Figure 5. The distance-calibrated Hubble diagram of a *complete* sample of spiral galaxies with TF distances and with $v_{220} < 1000 \text{ km s}^{-1}$. (a) Galaxies outside the Virgo region ($\alpha_{M87} > 30^\circ$). An apparently bright and an apparently faint galaxy and their respective individual Hubble constants H_i are shown. (b) Galaxies within the Virgo region ($\alpha_{M87} < 30^\circ$).

If the velocities v_0 (corrected only to the barycenter of the Local Group) were used instead of v_{220} one would obtain $H_0 = 59.0 \pm 2.9$ with slightly larger scatter.

3.2. The local distance-calibrated Hubble diagram from the TF relation

The Tully-Fisher (TF) relation (M_B^0 vs. 21-cm line width at 20% maximum intensity) can be calibrated via 29 sufficiently inclined spiral galaxies from Table 1. Two galaxies, NGC 5204 and 5585, can be added with half weight on the assumption that they lie as companions of NGC 5457 at the latter's distance. One obtains then

$$M_B^0 = -7.31 \log w_{20} - (1.833 \pm 0.095); \quad \sigma_M = 0.53. \quad (10)$$

The data of the individual galaxies are given by Federspiel (1999). The slope of the relation is taken from a complete sample of Virgo cluster members (Federspiel 1999) and is in very good agreement with the calibrators used here.

The calibration in equation (10) is applied to a (nearly) *complete*, distance-limited sample of inclined ($i \geq 45^\circ$) spirals with $v_{220} < 1000 \text{ km s}^{-1}$ and $|b| > 20^\circ$, as compiled by Federspiel (1999); Virgo and UMa cluster members are excluded as well as peculiar and HI-truncated galaxies. The resulting Hubble diagram of $\log v_{220}$ versus the TF distances of the 92 galaxies *outside* the Virgo region ($\alpha_{M87} > 30^\circ$) gives a mean value of $H_0 = 59.2 \pm 2.5$ (Fig. 5a); the large scatter of $\sigma_{(m-M)} = 0.86$ is presumably due to observational errors of the linewidths w_{20} , which are compiled from various sources. Yet the scatter of the 36 galaxies *within* $\alpha_{M87} < 30^\circ$ is still significantly larger ($\sigma_{(m-M)} = 1.18$; Fig. 5b). This can only be explained by the enhanced influence of peculiar

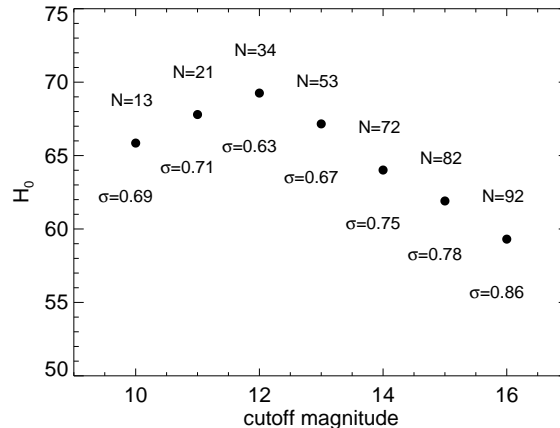


Figure 6. The local value of H_0 from TF distances ($\alpha_{\text{M87}} > 30^\circ$) in function of the cutoff magnitude of the galaxy sample. Incomplete samples give arbitrarily large values of H_0 .

motions in this dense region. In that case the 1000 km s^{-1} limit provides a fuzzy distance limit and the corresponding value of $H_0 = 45.3 \pm 4.3$ is unreliable.

The large scatter of the TF distances make the use of *complete*, distance-limited samples essential (cf. Fig. 6).

The statistical agreement of the local value of H_0 from Cepheids (Fig. 4) and the TF method (Fig. 5) is a tautology, – at least to the extent that the fewer Cepheids represent a fair sample with respect to the local expansion field. The bulk of the calibrators ($n = 31$) of the TF relation have also been used in Fig. 4 ($n = 23$), and the TF distances can hardly provide more than a consistency check.

Thus Section 3.2 sheds more light on the TF *method* than on the local value of H_0 . It is questionable whether other distance indicators (planetary nebulae, the $D_n - \sigma$ or fundamental plane method, surface brightness fluctuations) will ever do better for field galaxies – even if objectively selected samples will become available – than the TF method whose difficulties are apparent here.

3.3. The distance-calibrated Hubble diagram of local groups and clusters

Useful distance determinations of six local groups and clusters are compiled in Table 3. The Table is self-explanatory. However, one remark is in place concerning the Virgo cluster. The cluster has an important depth effect which has caused the *mean* cluster distance (i.e., the mean of subclusters A + B) to be controversial for a long time. The well resolved cluster spirals (Sandage & Bedke 1988) are expected to lie on the near side of the cluster; this expectation is born out for the majority of spirals with known Cepheid, SNe Ia or TF distances (Fig. 7). The Cepheid distances of NGC 4321, 4535, and 4548, which were selected on grounds of their high resolution can therefore not reflect the *mean* cluster distance.

Table 3. Distances of local groups and clusters

Group/Cluster	$\langle v_{220} \rangle$	μ^0	Method
South Polar gr.*	112	26.68 ± 0.20	Cepheids (1) ^a
M 101 gr.*	405	29.36 ± 0.10	Cepheids (1) ^a , TRGB ^f
Leo*	652	30.21 ± 0.05	SNe Ia (2) ^b , Cepheids (3) ^a , TRGB ^f
UMa [†]	1060	$\geq 31.33 \pm 0.15$	TF ^c , LC ^d
Virgo [‡]	1179	31.60 ± 0.20	SNe Ia (3) ^b , Cepheids (4) ^a , TF ^c , LC ^d , GC ^e
Fornax*	1338	31.60 ± 0.10	SNe Ia (3) ^b , Cepheids (3) ^a

* Group/cluster membership as defined by Kraan-Korteweg (1986)

† Two separate agglomerations can be distinguished in the UMa cluster; the nearer, presumably more nearly complete agglomeration with 18 TF distances is considered here (Federspiel 1999)

‡ Cluster membership as defined by Binggeli et al. (1993)

Sources: (a) Table 1; (b) SNe Ia calibration as in Section 5.4; (c) Federspiel (1999); (d) Luminosity classes (Sandage 2001); (e) Globular Clusters (Tammann & Sandage 1999); (f) Kennicutt et al. (1998)

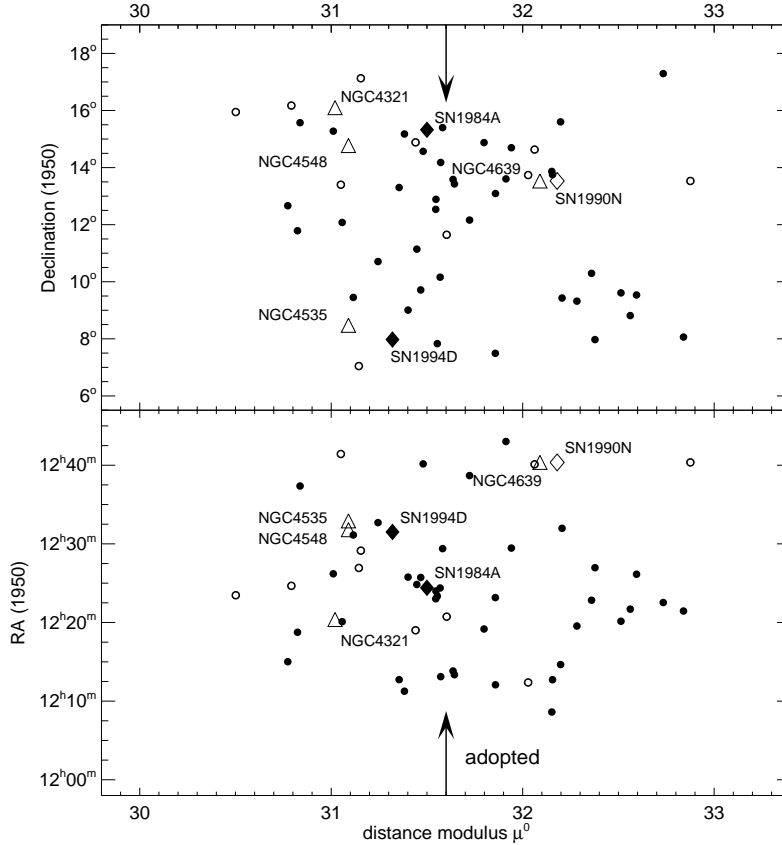


Figure 7. An illustration of the depth effect of the Virgo cluster. The position of cluster members is shown (declination [upper panel] and RA [lower panel] vs. μ^0) with known Cepheid (triangles), SNe Ia (diamonds), or TF (circles) distances. The majority of the well resolved galaxies (open symbols) lie on the near (left) side of the cluster.

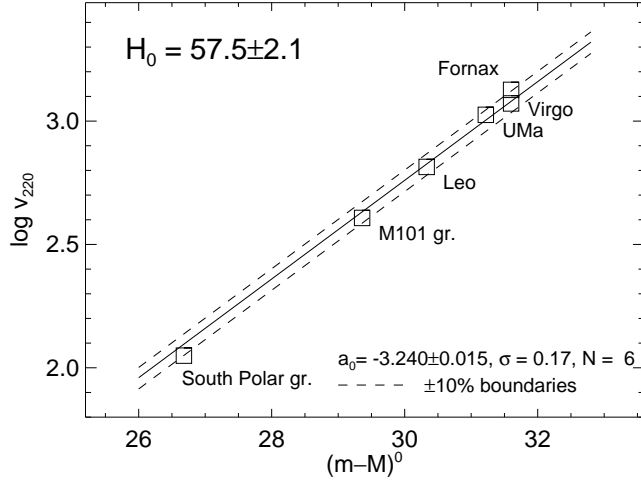


Figure 8. The distance-calibrated Hubble diagram for six local groups and clusters from Table 3.

The Virgo cluster distance from the peak of the luminosity function of globular clusters ($\mu^0 = 31.70 \pm 0.30$) is of particular interest because it is here the only distance independent of Cepheids, being based on only Population II objects (RR Lyr and Galactic globular clusters). Yet the method still lacks a theoretical understanding and does not seem to work for the Fornax cluster (Tammann & Sandage 1999).

The Hubble diagram of the six groups and clusters in Table 3 is shown in Fig. 8. Giving half weight to the nearby South Polar group (NGC 300) yields $H_0 = 57.5 \pm 2.1$.

The three determinations of the local value of H_0 in 3.1 to 3.3 give a weighted mean of $H_0 = 59.2 \pm 1.4$.

4. The Intermediate Expansion Field

For the determination of the *cosmic* value of H_0 the intermediate expansion field ($1200 \lesssim v_{220} \lesssim 10\,000 \text{ km s}^{-1}$) is irrelevant. The large-scale route through SNeIa is in any case superior and the most direct one (Section 5). Intermediate-size distances are only needed to study deviation from a smooth Hubble flow (e.g. the local CMB dipole motion). SNeIa are not yet useful here because of their paucity.

Distance determinations of field galaxies beyond $\sim 1200 \text{ km s}^{-1}$ are extremely difficult because of incompleteness bias. Elaborate parametric or non-parametric methods have been developed to correct for this bias (e.g. Theureau et al. 1998; Federspiel et al. 1998; for a compilation cf. Tammann et al. 2000; Hendry 2001). The conclusion is $50 < H_0 < 65$.

Nevertheless usefull Hubble diagrams of clusters have been established using *relative* cluster distances, which can be fitted to nearby clusters with known

distances (cf. Table 3) to yield distance-calibrated Hubble diagrams. (1) The Hubble diagram of first-ranked cluster galaxies by Sandage & Hardy (1973), if fitted to the brightest galaxies in the Virgo, Fornax (and Coma) clusters, gives $H_0 = 51 \pm 7$. (2) Giovanelli et al. (1997) and Dale et al. (1999) have provided TF distances of 71 clusters ($v < 25\,000 \text{ km s}^{-1}$), using about 10 galaxies per cluster. These clusters define an impressively tight Hubble diagram with a scatter of only $\sigma_{(m-M)} = 0.11$. Using the Fornax cluster as zero point one obtains $H_0 = 63 \pm 5$. (3) Relative $D_n - \sigma$ and fundamental plane distances have been derived for 10 clusters ($v < 10\,000 \text{ km s}^{-1}$) by Kelson et al. (2000). The ensuing Hubble diagram with $\sigma_{(m-M)} = 0.19$ combined with the Coma cluster distance gives $H_0 = 66 \pm 8$. For details see Tammann (2001).

The routes through (1) and (2) go beyond what we have defined as the “intermediate” expansion field and reflect already on the large-scale value of H_0 . It has been suggested (Sakai et al. 2000b) that method (2), if fitted to equation (10), leads to $H_0 \gtrsim 70$. This is, however, a grave error, because equation (10) can only be applied to distance- or volume-limited samples, while the relative TF distances of distant clusters are based on only a few subjectively selected cluster members.

5. The Cosmic Expansion Field

5.1. The Hubble diagram of blue SNe Ia out to $30\,000 \text{ km s}^{-1}$

A sample of 35 blue SNe Ia with good B , V (and I) photometry, $1200 \leq v_{220} \lesssim 30\,000 \text{ km s}^{-1}$, and $(B-V)_{\text{max}}^0 \leq 0.06$ has been compiled by Parodi et al. (2000). Their residual magnitudes (at maximum light) from a mean Hubble line correlate with the decline rate Δm_{15} and the color $(B-V)_{\text{max}}^0$. If these dependencies are removed one obtains corrected magnitudes $m_{B,V,I}^{\text{corr}}$, which define linear Hubble lines (corresponding closely to an $\Omega_m = 1$ model) of the form

$$\log v = 0.2 m_{B,V,I}^{\text{corr}} + c_{B,V,I} \quad (11)$$

with very small scatter $\sigma_{B,V} = 0^m 13$, $\sigma_I = 0^m 12$ (Parodi et al. 2000).

The small scatter is most remarkable because it can be accounted for by photometric errors alone, leaving very little room for peculiar motions ($v_{\text{pec}}/V_{220} < 0.06$) and luminosity variations of SNe Ia, once they are corrected for Δm_{15} and color. Yet the most important fact for the determination of H_0 is that the small scatter provides indisputable proof for blue SNe Ia (corrected for Δm_{15} and color) being by far the best distance indicators known, which at the same time makes them insensitive to selection bias.

Nine of the 35 SNe Ia are corrected for Galactic absorption by more than $A_V = 0^m 2$ (Schlegel et al. 1998). They lie significantly ($0^m 21 \pm 0.04$) above the mean Hubble line defined by the remaining 26 SNe Ia, presumably because their Galactic absorption is overestimated. The more reliable 26 SNe Ia with small Galactic absorption yield the following constant terms in equation (11)

$$c_B = 0.662 \pm 0.005, \quad c_V = 0.661 \pm 0.005, \quad c_I = 0.604 \pm 0.005 \quad (12)$$

with a reduced scatter of $\sigma_m = 0^m 11$ (!) in all three colors.

5.2. The luminosity calibration of SNe Ia

For nine local SNe Ia Cepheid distances are available (Saha *et al.* 2001). After standard corrections (Parodi *et al.* 2000) for Galactic and internal absorption and for decline rate Δm_{15} and color ($B - V$), they have the same intrinsic colors $(B - V)_{\max}^0$ as the distant SNe Ia. Their Cepheid-calibrated absolute magnitudes at maximum become (Saha *et al.* 2001):

$$\langle M_B^{\text{corr}} \rangle = -19.56 \pm .07, \langle M_V^{\text{corr}} \rangle = -19.53 \pm .06, \langle M_I^{\text{corr}} \rangle = -19.25 \pm .09. \quad (13)$$

5.3. The cosmic value of H_0

Transforming equation (11) gives

$$\log H_0 = 0.2 M_{B,V,I} + c_{B,V,I} + 5 \quad (14)$$

Inserting c from equation (12) and M from equation (13) yields $H_0(B) = 56.2 \pm 2.5$, $H_0(V) = 56.9 \pm 2.3$, and $H_0(I) = 56.8 \pm 3.1$.

If instead of a linear fit ($\Omega \approx 1$) the distant SNe Ia are fitted by an $\Omega_m = 0.3$, $\Omega_\Lambda = 0.7$ model (Carroll *et al.* 1992), the value of H_0 is marginally increased by 0.8 units, such that

$$\langle H_0(B, V, I) \rangle_{\text{cosmic}} = 57.4 \pm 2.3. \quad (15)$$

5.4. Other evidence for the large-scale value of H_0

Models of blue SNe Ia predict $M_B(\max) = -19.5(\pm 0.2)$ (Höflich & Khokhlov 1996; Branch 1998), which is in fortuitous agreement with the observed value in equation (13) which in turn leads to the value of H_0 in equation (15).

Distances have been derived for an impressive number of clusters from the Sunyaev-Zeldovich effect. Several reviews agree that the present data suggest $H_0 \approx 60$ (Mason *et al.* 2001; Rephaeli 2001; Carlstrom 2001).

The solution of H_0 from a single lensed quasar is degenerate as to the distance and lensing mass. Yet a combination of several such quasars restrict the solution to a rather narrow window near $H_0 \approx 55$.

The fluctuation spectrum of the CMB does not yet give stringent limits on H_0 , but values near $H_0 = 60$ are entirely consistent with multi-parameter solutions (Netterfield *et al.* 2001; Pryke 2001).

6. The Age of the Oldest Galactic Objects

The age test requires the oldest objects in the Universe to be younger than the expansion age. The latter becomes, with $H_0 = 60 \pm 5$, $\Omega_m = 0.3$, and $\Omega_\Lambda = 0.7$, $T = 15.7 \pm 1.5$ Gy. Various age determinations of very old objects in the Galaxy are available, e.g. Th or U ages of metal-poor stars (e.g. Cowan *et al.* 1999; Westin *et al.* 2000) or cooling times of White Dwarfs (for a compilation cf. Tammann 2001). The most stringent requirement comes probably from globular clusters. Sandage (1993) and Chaboyer *et al.* (2000) give 14.1 ± 1.5 and 11.7 ± 1.6 Gy, respectively, for several globular clusters (cf. also Gratton *et al.* 1997; Heasley *et al.* 2000; Sneden *et al.* 2000), but note that M 107 seems to

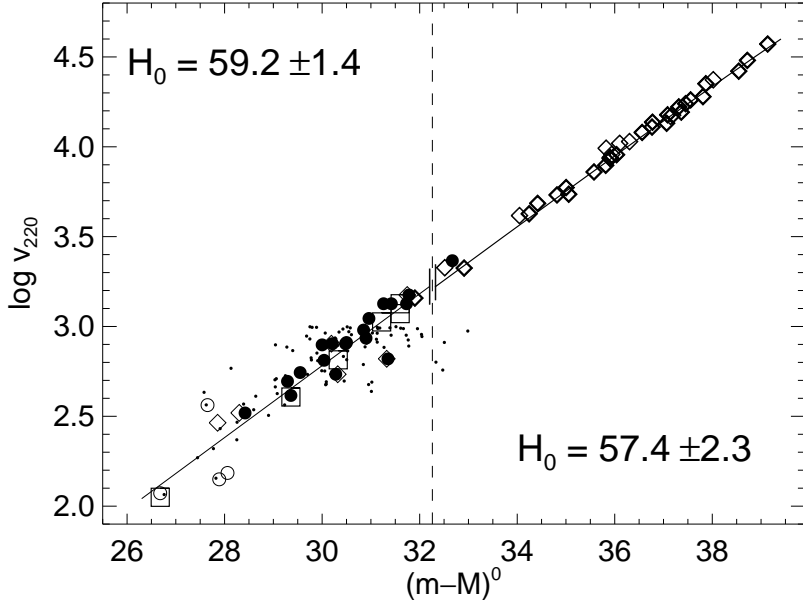


Figure 9. A synoptic distance-calibrated Hubble diagram extending over 11 magnitudes or a factor of 100 in recession velocity. The left-hand value of H_0 based on Cepheids (large dots), TF distances (small dots), and groups/cluster (squares) is independent of the right-hand value of H_0 based on SNeIa (diamonds), except that all distances rest ultimately on Cepheids. The full drawn line corresponds to $\Omega_m = 0.3$, $\Omega_\Lambda = 0.7$.

be older. If 14 ± 2 Gy is adopted for the latter, and if ~ 1 Gy is added for its gestation time, a cosmic age of 15 ± 2 Gy is required. This requirement is well met by the above expansion age.

7. Results and Conclusions

A synopsis of the distance determinations in Sections 3 and 5 is shown in Fig. 9. The distance moduli of the SNeIa are determined here from their apparent magnitudes $m_{B,V,I}^{\text{corr}}$ and the absolute magnitudes $M_{B,V,I}^{\text{corr}}$ in equation (13). The local expansion field extends into the cosmic expansion without any significant break.

If one chooses to base the Cepheid distances of the SNeIa-calibrating galaxies on the new P - L relations (eq. 7 & 8), they are reduced by 6% (cf. eq. 8), i.e.

$$H_0(\text{cosmic}) = 60.8 \pm 2.3. \quad (16)$$

For all practical applications $H_0 = 60$ can be used everywhere, except in nearby high-density regions.

So far only statistical errors have been quoted. It comes as a surprise that the largest source of systematic errors is in the *shape* of the P - L relation (6%), followed by the metallicity dependence of Cepheids and the photometric HST zero point in the crowded fields of SNe Ia-calibrating galaxies (4%). The zero point of the P - L relation, the slope of the Δm_{15} correction of SNe Ia and the HST photometry may each contribute systematic 2-3% errors. Systematic errors due to absorption corrections for the nearby, calibrating SNe Ia and the distant SNe Ia are negligible, because the two sets have closely the same colors ($\langle B - V \rangle = -0.01 \pm 0.01$; cf. Parodi et al. 2000). Unless there is a conspiracy of the individual systematic errors, the total systematic error is < 10%.

The resulting expansion age of $T = 15.7 \pm 1.5$ Gy ($H_0 = 60 \pm 5$, $\Omega_m = 0.3$, $\Omega_\Lambda = 0.7$) gives sufficient room for the oldest dated objects in the Galaxy.

Acknowledgments. The first three authors thank the Swiss National Science Foundation for financial support. G. A. T. and F. T. thank also the PRODEX programme of the Swiss Space Office for support.

References

Alibert, Y., & Baraffe, I. 2000, in: The Impact of Large-Scale Surveys on Pulsating Star Research, eds. L. Szabados and D. Kurtz, ASP Conf. Ser. 203, p. 250

Baraffe, I., & Alibert, Y. 2001, A&A, 371, 592

Binggeli, B., Popescu, C.C., & Tammann, G.A. 1993, A&AS, 98, 275

Branch, D. 1998, ARA&A, 36, 17

Caputo, F., Marconi, M., Musella, I., & Santolamazza, P. 2000, A&A, 359, 1059

Carlstrom, J.E. 2001, this Conference

Carroll, S.M., Press, W.H., & Turner, E.L. 1992, ARA&A, 30, 499

Chaboyer, B., Demarque, P., Kernan, P.J., & Krauss, L.M. 1998, ApJ, 494, 96

Chaboyer, B., Sarajedini, A., & Armandroff, T.E. 2000, AJ, 120, 3102

Chiosi, C., Wood, P.R., & Capitanio, N. 1993, ApJS, 86, 541

Cioni, M.-R.L., van der Marel, R.P., Loup, C., & Habing, H.J. 2000, A&A, 359, 601

Cowan, J.J., et al. 2000, ApJ, 521, 194

Dale, D.A., Giovanelli, R., Haynes, M.P., Camusano, L.E., & Hardy, E. 1999, AJ, 118, 1489

Feast, M.W. 1984, MNRAS, 211, 51

Feast, M.W. 1999, PASP, 111, 775

Feast, M.W., & Catchpole, R.M. 1997, MNRAS, 286, L1

Federspiel, M., Tammann, G.A., & Sandage, A. 1998, ApJ, 495, 115

Federspiel, M. 1999, Ph.D. Thesis, Univ. of Basel

Freedman, W.L., et al. 2001, ApJ, 553, 47

Giovanelli, R., et al. 1997, AJ, 113, 22

Girardi, L., & Salaris, M. 2001, MNRAS, 323, 109

Gould, A. 1994, ApJ, 426, 542

Gratton, R.G., et al. 1997, ApJ, 491, 749

Groenewegen, M.A.T., & Oudmaijer, R.D. 2000, A&A, 356, 849

Groenewegen, M.A.T., & Salaris, R.D. 2001, A&A, 366, 752

Heasley, J.N., et al. 2000, AJ, 120, 879

Hendry, M. 2001, this Conference

Herrnstein, J.R., et al. 1999, *Nature*, 400, 539

Höflich, P., & Khokhlov, A. 1996, *ApJ*, 457, 500

Kelson, D.D., et al. 2000, *ApJ*, 529, 768

Kennicutt, R.C., et al. 1998, *ApJ*, 498, 181

Kovács, G. 2000, *A&A*, 363, 1

Kraan-Korteweg, R.C. 1986, *A&AS*, 66, 255

Madore, B., & Freedman, W.L. 1991, *PASP*, 103, 933

Madore, B., & Freedman, W.L. 1998, *ApJ*, 492, 110

Mason, B.S., Meyers, S.T., & Readhead, A.C.S. 2001, *ApJ*, 555, L11

Netterfield, C.B., et al. 2001, *ApJ*, submitted (astro-ph/0104460)

Newman, J.A., et al. 1999, *ApJ*, 523, 506

Panagia, N. 1999, in: *New Views of the Magellanic Clouds*, eds. Y.-H. Chu, N. Suntzeff, J. Hesser, & D. Bohlender, IAU Symp. 190, p. 549

Parodi, B.R., Saha, A., Sandage, A., & Tammann, G.A. 2000, *ApJ*, 540, 634

Pont, F. 1999, in: *Harmonizing Cosmic Distance Scales in a Post-Hipparcos Era*, eds. D. Egret & A. Heck, ASP Conf. Ser. 167, p. 113

Pryke, C. 2001, this Conference

Rephaeli, Y. 2001, in: *Matter in the Universe*, ed. R. v. Steiger (Bern: ISSI), in press

Romaniello, M., Salaris, M., Cassisi, S., & Panagia, N. 2000, *ApJ*, 530, 738

Saio, H., & Gautschy, A. 1998, *ApJ*, 498, 360

Saha, A., Sandage, A., Tammann, G.A., Dolphin, A.E., Christensen, J., Panagia, N., & Macchietto, F.D. 2001, *ApJ*, 562, 314

Sakai, S., Zwitsky, D., & Kennicutt, R.C. 2000a, *AJ*, 119, 1197

Sakai, S., et al. 2000b, *ApJ*, 529, 698

Sandage, A. 1993, *AJ*, 106, 719

Sandage, A. 2001, *AJ*, in press (paper X of the Bias Series)

Sandage, A., Bell, R.A., & Tripicco, M.J. 1999, *ApJ*, 522, 250

Sandage, A., & Bedke, J. 1988, *Atlas of Galaxies*, (NASA: Washington)

Sandage, A., & Hardy, E. 1973, *ApJ*, 183, 743

Sandage, A., & Tammann, G.A. 1971, *ApJ*, 167, 293

Sasselov, D.D., et al. 1997, *A&A*, 324, 471

Schlegel, D., Finkbeiner, D., & Davis, M. 1998, *ApJ*, 500, 525

Sneden, C., et al. 2000, *ApJ*, 536, L85

Tammann, G.A. 2001, in: *The Century of Space Science*, eds. J. Blecker, J. Geiß, & M.C.E. Huber, (Dordrecht: Kluwer), in press

Tammann, G.A., & Sandage, A. 1999, in: *Harmonizing Cosmic Distance Scales in a Post-Hipparcos Era*, eds. D. Egret & A. Heck, ASP Conf. Ser. 167, p. 204

Tammann, G.A., Sandage, A., & Saha, A. 2000, in: *A Decade of HST Science*, eds. M. Livio, K. Noll & M. Stiavelli, (Cambridge: CUP), in press (astro-ph/0010422)

Tanvir, N.R., Ferguson, H.C., & Shanks, T. 1999, *MNRAS*, 310, 175

Theureau, G., Hanski, M., Ekholm, T., Bottinelli, L., Gouguenheim, L., Paturel, G., & Teerikorpi, P. 1997, *A&A*, 322, 730

Thim, F. 2001, Ph.D. Thesis, Univ. of Basel

Udalski, A., et al. 1999, *AcA*, 49, 201

Van Leeuwen, F., et al. 1997, *MNRAS*, 287, 955

Walker, A.R. 1992, *ApJ*, 390, L81

Walker, A. 1999, in: *Post-Hipparcos cosmic candles*, eds. A. Heck & F. Caputo, (Dordrecht: Kluwer), p. 125

Westin, J., Sneden, C., Gustafsson, B., & Cowan, J.J. 2000, *ApJ*, 530, 783